4.0 INFLUENCE OF THE THERMAL ECOLOGY OF LOCUSTS AND GRASSHOPPERS ON THE SPATIAL VARIATION OF PERFORMANCE OF AN ENTOMOPATHOGEN.

ABSTRACT

1. A model has been developed to predict the performance of a *Metarhizium*–based biopesticide against locusts and grasshoppers. Currently, the model is limited to predicting rate of mortality at site-specific locations. The main aim of this chapter is to enhance the utility of this model by linking it with meteorological station data in a Geographic Information System (GIS) framework and use it to investigate the spatial variation in the performance of *Metarhizium anisopliae* var. *acridum* in controlling locusts and grasshoppers. Examples of pathogen performance against five economically important pest species (*Dociostaurus maroccanus* in Spain, *Locustana pardalina* in South Africa, *Oedaleus senegalensis* in Niger, *Nomadacris septemfasciata* in Zambia and *Chortoicetes terminifera* in Australia) were used to illustrate the spatial variation in the rate of mortality within a country.
2. Differences in daily mean maximum and minimum ambient temperatures recorded at the field site and at meteorological stations can vary by 5-15°C and 0-9°C, respectively. Disparity in maximum temperature was overcome by capturing the spatial variations in the thermal ecology of locusts and grasshoppers through the recalibration of body temperatures to meteorological station data. Species-specific body temperature models successfully described hourly body temperature ($R^2 > 0.56 – 0.87$). GIS mortality estimates, when compared with observed field data, successfully predicted when 90% mortality would occur to within 5 days.
3. The model was used to further test model accuracy against an additional four data sets for three of the above species and one new species, the Desert locust *Schistocerca gregaria* in Mauritania. Model predictions were also accurate to within 5 days.
4. The GIS model can be used with confidence to investigate area-wide spatial variation in the performance of a biopesticide and used to assess management strategies of locust control.

4.1 Introduction

In 1997, the FAO (Food and Agriculture Organisation of the United Nations) approved the use of Green Muscle®, *Metarhizium anisopliae* var. *acridum*-based biopesticide, for use in conservation and environmentally sensitive areas against locust and grasshopper pests in South Africa and the CILSS (Comité permanent Inter-états pour la lutte contre la sécheresse dans le Sahel) countries (includes Burkina Faso, Mali, Mauritania, Niger, Senegal, Chad, Gambia, Cape-Verde and Guinea-Bissau) (see Thomas *et al.*, 2000 for overview). Operational use of this product, as an alternative to chemical pesticides, has however been minimal with some continuing field trials. This can be attributed to both production constraints and the perception that the biological control agent is unreliable.

Body temperature of the host critically determines the rate of *Metarhizium* development and hence, speed of kill by the pathogen against locusts and grasshoppers. This can lead to considerable variation in mortality rates across space and time. For example, in environments with warms nights around 20-25^{o}C (i.e. conducive for *M. anisopliae* growth), combined with relatively short days (limiting the number of thermoregulation hours by the locust), 50-100% mortality can be achieved in less than 15 days (e.g. Lomer *et al.*, 1997b; Langewald *et al.*, 1999; Hunter *et al.*, 2001). On the other hand, in regions where day length is longer, providing considerable thermoregulatory opportunity for the host, and nights are cold (15^{o}C at which pathogen growth is very slow), 50% mortality may take longer than 35 days with some individuals surviving well into reproductive maturity (Arthurs & Thomas, 2000). Therefore the key to using the biopesticide effectively is to predict how the pathogen will perform across space and time. In Chapter 3, a model was developed to predict the performance of a *Metarhizium*–based biopesticide against locusts and grasshoppers. Currently, the model is limited to predicting rate of mortality using data collected at site-specific locations. This study extends the utility of this model using meteorological station data in a geographic information system (GIS) to investigate the spatial variation of pathogen-performance, against a number of economically important locust pest species that are currently the subject of on-going field trials using *Metarhizium*–based biopesticides.

Several studies have successfully mapped spatial and/or temporal abundance of vector-borne diseases and/or insect pest incidences using environmental data

through satellite images. For example, Rogers and Randolph (2000) illustrated changes in malaria distribution with climate change. Similarly, Voss and Dreiser (1994) successfully mapped locust habitats. Remotely sensed data coupled with distribution of locust populations has been extensively used to describe environments favourable for the outbreak of several important locust and grasshopper species (see Nailand, 1993 for summary). Many of these studies have mainly used vegetation classification or normalized differential vegetation index as proxies for temperature and soil moisture to describe known distribution of pests and diseases. However, the *Metarhizium*-performance model (see Chapter 3) is based on hourly pathogen development, a temporal scale for which the remotely sensed data are captured is too coarse a measure to provide accurate estimates. Patz *et al.*, (1998) and Shaman *et al*., (2002) found that prediction of malaria transmission and mosquito abundance could be improved when simulated hourly meteorological data variables coupled with hydrological models were used. Here we use hourly temperature surfaces coupled with biological models to investigate spatial performance of the biopesticide in a GIS framework.

In general, temperature is collected at meteorological stations that are geographically scattered throughout a region. Numerous models predicting temperature across space (e.g. interpolation techniques predicting temperature at unsampled points between meteorological stations (see Collins & Bolstad, 1996; Jarvis & Stuart, 2001a, b for review)) and time (e.g. hourly intervals using a sine-curve method (Parton & Logan, 1981)) have been developed. The accuracy of these techniques can be variable and are largely influenced by the data [e.g. distribution of stations (clustered v.s. scattered points) and accuracy of the data itself], spatial variability of the landscape [(topography) (MacEachren & Davidson, 1987)], temporal scale (hourly v.s. daily v.s. monthly), spatial scale (regional v.s. continental), and computing power.

Several studies have compared the effectiveness of different spatial interpolation techniques for predicting temperature (see Collins & Bolstad, 1996; Jarvis & Stuart, 2001a, b for reviews). Jones and Gladkov (1999) created accurate monthly temperature surfaces using the inverse-distance-weighting (IDW) corrected by the lapse rate method at the continental level for Latin America and Africa. These surfaces have subsequently been used in a number of agricultural applications (e.g.

guiding and investigating taxonomic and genetic variation of wild plants (Jones *et al.*, 1997; Jones & Gladkov, 1999)), and so form the basis of the method used here.

Collecting hourly ambient temperatures across a range of microhabitats at different field sites can be time-consuming and expensive. Therefore models have been developed to predict temperatures based on daily minimum and maximum air temperature recorded at meteorological stations (e.g. Parton & Logan, 1981; Cesaraccio *et al.*, 2001 for literature reviews). Parton & Logan (1981) developed a sine-exponential model that produces accurate results of hourly temperatures within and between seasons (Wann *et al.*, 1985) and has been extensively used for agricultural crop models (e.g. Porter *et al.*, 2000). However, an important consideration when using temperatures recorded at weather stations are that they may not be representative of temperatures of the microhabitat at the field site (Kennedy, 1997; Bryant & Shreeve, 2002). This variance can be attributed to the fact that air temperatures are recorded in protected environments (often Stevenson's screen) at heights of 1-2m above the ground surface at meteorological stations, where temperatures are less variable than those found occurring nearer the soil surface (Arya, 1988; Kennedy, 1997), and tend to be relatively cooler than microhabitats occupied by most insects including locusts and grasshoppers. For example, temperatures at the soil surface maybe 15-20°C hotter than air temperatures at 15cm and as much as 25-30°C at 150cm (height at which meteorological temperature data are recorded) above the soil surface (see Figure 1, data from Castuera, Southern Spain). This discrepancy can lead to gross inaccuracies when determining temperatures actually experienced by insects and thus, the outcome of processes dependent on temperature rate effects (e.g. distribution of insects (Bryant *et al.*, 2002) and invasive species (Drake, 1994); global warming effects on disease risk (Harvell *et al.*, 2002; Rogers & Randolph (2000)). Incorrect predictions may be further accentuated when insects thermoregulate, maintaining their body temperatures at temperatures different to those recorded both in the field and at meteorological stations (see Chapter 2).

Many ectotherms, including the majority of locusts and grasshoppers are able to maintain body temperatures that are independent from their surroundings (e.g. Digby, 1955; Heinrich, 1974; Uvarov, 1977; May, 1979 for reviews). For example, *Locustana pardalina* (Walker), as with other economically important acridid species

(e.g. see Uvarov 1977; Chapter 2), is an active behavioural thermoregulator, able to regulate its body temperature close to 40°C for at least 8 hours of the day (Blanford & Thomas, 2000) and can result in body temperatures being as much as 10-15°C higher than ambient temperatures. The thermal behaviour of *L. pardalina*, as with many insects, has been successfully described through the use of body temperature models, which capture changes in body temperature throughout the day in relation to ambient temperature and other environmental factors, such as solar radiation (e.g. Kemp, 1986; Carruthers *et al.*, 1992; Blanford & Thomas, 2000; Bryant *et al.*, 2000; Chapter 2). Therefore, instead of concentrating on quantifying thermal features of different microhabitats, as proposed by Kennedy (1997), this study quantifies the known behaviour of several locust and grasshopper species in relation to ambient temperature recorded at meteorological stations, which can then be substituted into the *Metarhizium*-performance model to predict the rate of mortality by this biopesticide.

4.2 Materials and Methods

Overview

This study investigates the spatial variation of mortality by *M. anisopliae* var. *acridum* against five economically important pest species that are the subject of on-going field trials. The species investigated are: *Locustana pardalina* from the Karoo biome of South Africa; *Oedaleus senegalensis* from Sahelian Niger in West Africa; *Nomadacris septemfasciata* from southern Africa and currently being studied in both Tanzania and Zambia; *Dociostaurus maroccanus* from northern Africa and the Mediterranean basin' and *Chortoicetes terminifera* from Southeastern Australia. Mortality predictions for *Schistocerca gregaria* in Mauritania will also be used to assess model accuracy. Model simulations are run simultaneous to field trials conducted within each region and compared to observed mortality.

4.2.1 Meteorological Station Data

Daily minimum and maximum temperature data collected at meteorological stations around the world were obtained from the National Climate Data Center (NCDC) website (http://www.ncdc.noaa.gov/). Data points for all locations contained latitude, longitude, daily minimum temperature, daily maximum temperature and mean daily temperature. Wind speed and total number of sunshine hours were not consistently recorded at all stations and were therefore eliminated.

All points were quality checked for missing data. Records were removed if both the daily mean and daily minimum (or maximum) temperature data were missing, otherwise for missing values the daily minimum or maximum temperature was calculated using the daily mean and daily minimum or maximum values. Meteorological stations were removed (i) when less than 7 days of temperature data was recorded during a single month and (ii) when 5 consecutive days of temperature data were missing. For days with missing minimum or maximum temperature values, new temperature values were estimated by interpolating between missing days. Meteorological station points were imported directly into a GIS system – ArcView 3.2 (ESRI^{TM}).

4.2.2 Simulated hourly temperature values

The sine-exponential model proposed by Parton and Logan (1981) assumes that maximum temperature occurs during daylight hours and minimum temperature during the early hours of the morning (just before sunrise). Daytime variations of temperature (T_{day}) are described by a truncated sine wave (Eq. 1), while nighttime temperatures (T_{night}) are determined by an exponential function (Eq. 2).

$$T_{day} = (T_{max} - T_{min})\sin\left(\frac{\pi m}{Y + 2a}\right) + T_{min} \qquad \textbf{[Eq 1]}$$

$$T_{night} = T_{min} + (T_{sunset} - T_{min})\exp -\left(\frac{bn}{Z}\right) \qquad \textbf{[Eq 2]}$$

T_{max} is daily maximum temperature (°C), T_{min} is daily minimum temperature (°C), T_{sunset} is the temperature recorded at sunset (°C), m is the number of hours after the occurrence of minimum temperature until sunset (h), n is the number of hours after sunset until the time of the minimum temperature (h), Z is the night length (h) and Y is the day length (h). Time of sunrise and sunset vary seasonally and geographically. These were calculated based on latitude, longitude, time zone and date, for each location using astronomical algorithms of Meeus (1999), programmed into Microsoft Excel v. 10.

Two parameters (where a is the lag coefficient for the maximum temperature and b is the night-time temperature coefficient) control the rate of temperature

increase and decrease. An additional parameter, *c*, determines the lag time of minimum temperature from the time of sunrise.

4.2.2.1 Sine-curve parameters

The rate at which temperature increases and decreases varies with height (both above the soil surface (see Figure 1) and elevation), vegetation and moisture. The parameters for the sine-curve (*a*, *b* and *c*) vary as a function of height, location, habitat (Reicosky *et al.*, 1989) and day length. Incorrect parameterization can lead to inaccurate temperature estimates (see Figure 2), as illustrated by a number of studies (see Reicosky *et al.*, 1989; Cesaraccio *et al.*, 2001; Snyder *et al.*, 2001). For example, in Figure 2, a 10°C difference in predicted temperature can occur when using sine-curve parameters that describe dry subtropical desert conditions as found in the Karoo, South Africa, with temperatures representative for humid tropical regions in Zambia or coastal zones. Therefore parameters were selected that adequately describe the thermal qualities of the environment investigated.

Parameters were derived by fitting sine-curves to daily minimum and maximum mean ambient temperatures collected at the field site. These were determined from temperature data collected daily on loggers at the field site (see Section 2.2.3, Chapter 2). Parameters were then used with daily minimum and maximum meteorological station data to estimate hourly temperature.

4.2.3 Error analysis

Accuracy of fit for each location was assessed by comparing predicted with observed temperature curves by determining the absolute mean error (*AME*) (Eq. 3), which is defined as the sum of the absolute value of difference between observed and predicted temperature for a defined period of time, and the overall accuracy of the slope of the curve was determined by the root mean square error (*RMS*) (Eq. 4) (see Parton & Logan, 1981; Reicosky *et al.*, 1989; Cesaraccio *et al.*, 2001).

$$AME = \frac{\sum_{i-1}^{n} \left| (X_i^s - X_i^0) \right|}{N} \qquad \textbf{[Eq 3]}$$

$$RMS = \sqrt{\frac{\sum_{i-1}^{n} (X_i^s - X_i^0)^2}{N}} \qquad \textbf{[Eq 4]}$$

where N = total number of hourly observations, n = hourly observations, X_i^0 = predicted temperature for ith observation, and X_i^s = observed temperature for the ith observation. Small values of RMS and AME denote greater accuracy since they indicate that predicted temperatures closely resemble observed temperatures, while larger values indicate greater deviations of predictions from observed values.

4.2.4 Interpolating daily minimum and maximum temperature

Minimum and maximum temperature surfaces were created with a 10-km cell resolution, and an inverse-distance-interpolate (IDW) using the five nearest stations (Eq. 5). Temperature surfaces were standardised for elevation [Digital Elevation Model (DEM) downloaded from the USGS website (USGS, 1999)] using a lapse rate model (Eq. 6).

$$Ta_{met} = \frac{\sum_{i=1}^{n}(x_i) \bullet d_{ij}^{-r}}{\sum_{i=1}^{n} d_{ij}^{-r}} \qquad \textbf{[Eq 5]}$$

$$Ta_{new} = Ta_{met} - (L * \nwarrow h) \qquad \textbf{[Eq 6]}$$

Where Ta_{met} is the daily minimum or maximum temperature surface created using IDW, x_i are the station points, x_j are the points where the surface is to be interpolated, d^{-r} is the distance weighting power of 2, L = lapse rate (6°C/1000m), $\nwarrow h$ is the difference between the elevation at a location and the nearest meteorological station and Ta_{new} is the corrected daily minimum and maximum temperature surface used to create hourly temperature surfaces (see Section 4.2.2).

4.2.5 Recalibration of body temperature models

In order to overcome differences in temperatures recorded in the field and at the meteorological station, body temperature models for the five study species (developed in Chapter 2) were recalibrated with meteorological station data. Ambient temperature was simulated at 1-minute intervals based on meteorological station minima and maxima. These simulated temperatures were matched to body temperatures taken at the same time and used to derive new body temperature models using a sigmoid model (see Section 2.2.2, Chapter 2; Section 3.2.2 (i), Chapter 3 for

methodology). Model accuracy is compared with predictions of body temperature models from Chapter 2 (see Chapter 2, Tables 2a and 3). For this study body temperature models for *L. pardalina, D. maroccanus, N. septemfasciata, O. senegalensis, C. terminifera* and Generic Model A were recalibrated and used to investigate the performance of *M. anisopliae* var. *acridum* in the field. Body temperature model for *S. gregaria* is not available therefore since this species is known to thermoregulate, maintaining body temperatures in the range of 38-40°C (Stower & Griffith, 1966), the generalised body temperature model (Model A) (see Chapter 2) was used to predict body temperatures for this species in the field.

4.2.6 Predicting the rate at which 90% mortality by Metarhizium anisopliae *var. acridum will occur*

Predicted locust body temperatures were substituted into the *Metarhizium*-performance model (see Chapter 3). Daily pathogen growth was calculated for each grid cell and evaluated for mortality events. Mortality occurred when the accumulated pathogen growth equalled 1 (equivalent to 90% population reduction). Grid cells containing a mortality event were assigned the day number after application, where the first 24 hours is considered day 0. Simulations were run for a total of 30 days with exception to *L. pardalina,* which was run for a total of 60 days. Start dates for each simulation were in accordance with field trials. Accuracy of model predictions for *L. pardalina, O. senegalensis,* and *N. septemfasciata* were compared with empirical field trial data (see Chapter 3, Table 3). For cases where empirical field trial data were absent, such as *D. maroccanus,* model predictions using meteorological station data were compared with those made using the field data (see Chapter 3, Table 4).

4.3 Results

4.3.1 Meteorological versus field daily minimum and maximum temperatures

Meteorological stations were within 5-50km of the field site for all cases with exception of Castuera, Spain, where the closest source of climate data was 110 km and Zambia where climate data was only available from Lusaka airport, approximately 220 km from Namwala the field site.

Figures 3a-d illustrates the distribution of meteorological stations with data available within each of the regions. In Niger, stations were located to the south of

the country along the border of Nigeria, Benin and Burkina Faso with little to no data available to the north and east of the country. In Zambia, meteorological data were only available from one source – Lusaka airport, which may not be representative of the wetland areas of the field site. To further add to this problem, no data were available to the north and west of the country, from surrounding countries such as Angola, Democratic Republic of Congo, and Tanzania. Data were available for Zimbabwe and Malawi. In comparison, in South Africa, Spain and Australia, meteorological stations were distributed relatively evenly throughout the country. Stations tended to be sparsely distributed in regions that were mountainous and lowly populated and more clustered in locations with higher populations. Interpolated temperature surfaces contained banding effects in regions where meteorological stations were sparsely distributed.

Mean daily minimum and maximum temperatures recorded at the field sites and at the nearest meteorological station varied. Differences in mean daily maximum temperature varied in excess of 15°C while daily mean minimum temperatures varied between 0-7°C (see Figure 4). Variations in daily mean maximum temperatures were greatest in Australia, where temperatures recorded in the field were ~40°C in comparison to ~25°C recorded at the meteorological station, resulting in a ~15°C difference. Daily mean minimum temperature differences were greatest in Australia and South Africa and were found to vary by as much as 6-8°C Differences between temperatures recorded at the field site and at meteorological stations were smallest (e.g. 0-3°C) during days when diurnal temperature ranges in the field were also small (e.g. $Ta < 11$°C).

4.3.2 Simulation of hourly minimum and maximum field temperatures

Humid zones, such as in Zambia and during the wet season in Niger, where mean minimum temperatures remain at or close to 20°C, followed a u-shaped pattern of heating and cooling (see Figures 5a-b). Temperatures in the field increased and decreased rapidly in the mornings (1.0-2.5°C/hr) and afternoons (1.2-1.5°C/hr), reaching maximum temperature between 12:00-14:00 hours. After sunset (between 18:00-19:00hr) temperatures were found to decrease a total of ~1-5°C (0.1-0.4°C/hr) until the time of minimum temperature, approximately 5 am. In comparison, temperature patterns in semi-arid desert regions, such as in the Karoo, South Africa, Central-western Spain and Southeastern Australia (see Figures 5c-e) were more

variable. Temperatures increased rapidly in the mornings at a rate of 2.7-3.7°C/hr reaching maximum temperatures between 12:00-14:00 hours and decreased at a rate of 1.2-1.6°C/hr in the afternoon until the time of sunset. However, unlike Zambia and Niger, temperatures continued to decrease rapidly (7-11°C in total: 0.6-0.9°C/hr in the Karoo; 11-16°C in total: 1.0-1.6°C/hr in Spain; and 4-7°C in total: 0.4-0.6°C.hr in Australia) until the time of minimum temperature, again at 5 am.

Different rate of temperature increase and decrease between the environments were successfully captured using three sine-curves. These include warm zones with minimum ambient temperatures remaining close to and above 20°C (a=1, b=5, c=-0.1) (see Figures 5a-b); semi-arid desert environments with minimum temperatures less than 20°C and a day length of 12-13 hours (a=1, b=1, c=-0.1) (see Figures 5c, 5e), as illustrated in South Africa and Australia. For regions where day lengths were extended and in excess of 14 hours, such as in Spain, a different set of parameters were required (a=2.2, b=2.5, c=-0.1) (see Figure 5d).

Table 1 shows the mean statistics obtained by comparing hourly temperature estimates with observed hourly temperature data for each of the locations. In general, the sine-curve parameters adequately captured temperature fluctuations, with a slope (b) of the regression line close to 1.0 and intercepts ranging from -0.641 (Niger) and 1.394 (South Africa). The R^2 value ranged from a low 0.84 for Zambia to 0.98 for Niger. Root mean square errors (RMS) were smallest for Niger (1.096) and largest for Spain (2.291) followed by Zambia (1.963) (Table 1). Greatest absolute hourly mean error (AME) occurred in Spain (AME ~1.6°C (Table 1)) but remained small in Niger (AME < 1°C).

For Niger, errors were greatest mid-morning (~10:00 am) and during the afternoon and early evening (Figure 5a). In Zambia deviations between observed and predicted temperatures were greatest during times of precipitation (e.g. Day 1) and cloud-cover (Day 3), otherwise simulated temperatures adequately captured temperature fluctuations (see Days 2 and 4) (Figure 5b). In South Africa errors were consistently high in the morning and during times when temperatures dropped possibly due to precipitation (e.g. Day 1) (see Figure 5c). In Spain errors were greatest shortly after sunrise and late afternoon until the time of sunset (Figure 5d). For Australia, errors were greatest at or close to sunset (Figure 5e).

4.3.3 Re-calibrated body temperature models

Daily diurnal range in meteorological ambient temperature was less than field derived ambient measurements (e.g. 16-32°C vs. 11-43°C in South Africa; 24-34°C vs. 23-41°C in Niger), which resulted in an increased range of body temperatures occurring for a single ambient temperature (see Figures 1a, b, d, e, Chapter 2 vs. Figures 6a-d). Body temperature parameter estimates for each of the five species and the generalised body temperature model (Model A) are shown in Table 2 with R^2 ranging from 0.56 to 0.87.

In general, the re-calibrated body temperature models adequately captured hourly body temperature fluctuations for each of the four species, with a slope (b) of the regression line close to 1.0 (0.859 – 1.003) and intercepts ranging from -0.226 (*O. senegalensis*, Niger) to 4.244 (*L. pardalina*, South Africa). The R^2 value ranged from a 0.70 for *N. septemfasciata*, Zambia, to 0.92 for *C. terminifera*, Australia. Body temperature estimates against meteorological temperatures found that all species, including generic Model A, had an absolute mean error (AME) within 2.4°C (1.85°C (*D. maroccanus*) to 2.32°C (*N. septemfasciata*) (Table 3)). Root mean square errors (RMS) were within 3.2°C with greatest errors for *C. terminifera* (RMS ~ 3.15°C) and smallest errors for *O. senegalensis* (RMS ~ 2.78) (Table 3).

Figure 7a-d illustrates simulated body temperatures based on temperatures collected at the field site to recalibrated body temperature estimates based on simulated meteorological station temperatures. Differences in body temperature estimates during daylight hours were greatest for *N. septemfasciata*, due to cloud cover and the occurrence of precipitation at the field site (Figure 7b); while for *O. senegalensis*, recalibrated body temperature estimates under-predicted maximum body temperatures throughout daylight hours by 3-5°C (see Days 1, 2, and 4, Figure 7a). Recalibrated body temperature estimates for both *L. pardalina* and *D. maroccanus*, during daylight hours, were similar to those predicted at the field site (Figure 7c-d) with the greatest errors occurring between the hours of sunrise and 12-noon. Body temperature estimates for *C. terminifera* had a tendency to underestimated daytime maximum body temperatures by 3-5°C.

Disparity between night-time body temperature estimates using meteorological station data and field data can vary by as little as 1-2°C (e.g. Day 2 (Figure 7a); Day 3 (Figure 7d)) to as much as 5-6°C (e.g. Day 1 and 2 (Figure 7c)).

This can be attributed to differences in night time temperatures recorded at the field site and at the meteorological station.

4.3.4 Pathogen-performance

Mapped outputs clearly illustrate spatial variation in the performance of *M. anisopliae* var. *acridum* in achieving 90% mortality within each country (see Figures 8a-e). The rate at which 90% mortality was predicted to take ranged from as little as 10 days in some regions within each country and could take in excess of 30 days in others. For example, in South Africa, during the field season of 1998, 90% mortality against *L. pardalina* was predicted to occur the fastest (< 20 days) in areas near the coast and to the south of the Drakensberg mountains (Figure 8c) with slower rate of mortality (> 30 days) occurring in the central and western regions of the country. Throughout the main locust problem areas in the semi-desert shrub lands of the Karoo, mortality was predicted to take as little as 21-25 days, in the areas near Upington, Marydale and Prieska; 26-29 days near Britstown and in excess of 30 days near Brandvlei and Vanwyksvley; resulting in a 9 day difference between the locust regions. Mortality predictions, when compared with field trial results found that the model under-predicted the rate of mortality by 29 days (Table 4).

In comparison, mortality against *O. senegalensis* was predicted to occur substantially faster throughout Niger with the speed of kill varying by 11 days (range 10 – 20 days) (Figure 8a). Mortality was found to occur fastest in the southern regions, close to borders of Burkino Faso, Benin and Nigeria, and became progressively slower to the North of the country. In Maine-Saroa, 90% mortality was predicted to occur in 16 and 15 days during 1996 and 1997, respectively. When compared with field trial results model predictions underestimated time to death by 5 days during 1996 and was in agreement during 1997 (Table 4).

The time taken to achieve 90% mortality against *D. maroccanus* was variable across Spain, ranging from 11 days to in excess of 30 days during 2000 (Figure 8d). Mortality was predicted to take as little as 11-15 days in the south, near Almeria, North of the *Sistema central*, along the coast of the Atlantic Ocean, and East of Zaragoza. Throughout the northern regions mortality estimates were predominately found to take between 16 and 20 days while in the southern and parts of the northeastern region mortality was predicted to take in excess of 30 days. This final

region included three of the four locust outbreak regions (e.g. Castuera, Ciudad Real and Zaragoza). At this time it is unclear how accurate mortality predictions are since field trial results are currently unavailable. However, when compared with mortality estimates made using site-specific data earlier (see Chapter 3) the GIS model was able to predict mortality to within 2 days (see Table 4).

Simulations against *N. septemfasciata* in Zambia indicated that control for this entire region would be relatively quick with mortality predictions taking less than 11 days (Figure 8b). This pattern suggests *M. anisopliae* var. *acridum* could be used throughout this region with great success. GIS mortality predictions when compared with observed field mortality at the 90% level were found to underestimate the rate of mortality by 2 days.

Throughout Australia the rate of predicted mortality against *C. terminifera* was predominantly found to take between 26-29 days (throughout the central northern regions) and in excess of 30 days throughout the south. Along the eastern region mortality was found to be more varied, with mortality taking between 11 and 25 days with large areas falling in the 11-15 day category. In the locust areas of Hay and Hillston, mortality was predicted to take 18 and 22 days respectively. When compared with mortality observed in the field, the model underestimated the rate of mortality by 1 day for Hay (Table 4).

Table 5 illustrates the accuracy of the temperature-dependent *Metarhizium*-performance model when further tested against three of the above species (e.g. *O. senegalensis* (1995), *L. pardalina* (1995) and *N. septemfasciata* (1997)) and one additional species (*S. gregaria* (1995)). Mortality predictions were accurate to within 5 days; ranging between 0 (*N. septemfasciata*) to 5 (*L. pardalina*) days. For *S. gregaria* mortality predictions were found to resemble those found in the field with an error of 2 days.

4.4 Discussion

Growing concerns of the impact of climate change on natural and managed ecosystems has lead to increased use of climate mapping techniques to investigate ecology of animal, plants and humans to potential risk of parasites and disease (see Clark *et al.,* 2001; Sutherst, 2001 for overview). Improved understandings of population dynamics of pests and transmission of diseases can be achieved through

the analysis of processes at various scales (e.g. field level to continental to global) within a landscape. Geographic Information Systems (GIS) coupled with remotely sensed data, environmental and socio-economic information are increasingly being used to visualise, explore and analyse existing and potential area-wide problems across spatial and temporal scales to provide, not only, an improved understanding of the processes contributing to population and disease dynamics (see Hajek *et al.,* 1993; Brewster *et al.,* 1999; Weseloh, 2003); but also used for research and implementation of control (e.g. Malaria information system in South Africa (Martin *et al.,* 2002); monitoring and forecasting (e.g. Desert locust (Healey *et al*., 1996) and for assessing risk of establishment of new introduced species (Sutherst, 1991)).

The methods presented here provide a basis for predicting the dynamic changes in efficacy of a biopesticide and is designed to predict the rate of mortality by *M. anisopliae* var. *acridum* against locusts and grasshoppers. The main aim of this work was to increase the utility of the *M. anisopliae* var. *acridum* biopesticide model by linking it to meteorological station data and moving beyond site-specific predictions. To this end, the model was incorporated into a GIS framework that enabled predictions to be made at a regional scale and enabled for the model to be further tested against an additional four data sets including one new species (1x *O. senegalensis*, 1x *L. pardalina*, 1x *N. septemfasciata* and 1x *S. gregaria*). Model predictions, at the 90% level, were found to be accurate to within 5 days for 8 of the 10 of the cases. Errors for the remaining cases had a tendency to underestimate the speed of kill, thus predicting that the rate of mortality would be achieved at a faster rate than actually was observed in the field. Three potential sources of errors were identified. These include; the availability and reliability of meteorological station data; errors associated with the simulation of daytime temperatures; errors associated with the recalibration of body temperature models.

Climate data recordings throughout the different regions varied spatially and temporally with some regions consistently containing reliable data (e.g. Spain and Australia) and others not (e.g. throughout much of Africa). This may be due to limited resources (i.e. lack of funds) and political instability (e.g. The Democratic Republic of the Congo and Angola). Thus, errors associated with daily minimum and maximum temperature surfaces can be attributed to several factors, such as accuracy of the raw data itself, missing temperature records and the result of interpolating between

sparsely distributed station networks. Errors may further be accentuated in environments with highly changeable weather patterns (i.e. resulting in highly fluctuating temperature changes) and/or regions that have variable topography (i.e. due to changes in inversion and lapse rates (see Collins & Bolstad, 1996 for overview)). In regions where weather patterns are more stable (i.e. temperatures continually oscillate between a set-point (e.g. 20°C to 35°C in Niger or Zambia)) and topography is similar, interpolating between a sparsely distributed network of stations may be less problematic.

Differences in maximum temperatures recorded at the meteorological station and at the field site were overcome through the use of recalibrated body temperature models; instead differences in minimum temperatures was found to have the greatest effect on the accuracy of model outcomes, as illustrated in South Africa against *Locustana pardalina* during 1998. Initial model simulation predicted mortality would take 30 days, under estimating the speed of kill by 29 days. When the data was analysed more closely it was found that a 5-6°C difference in minimum temperature, (see Figure 8c on Days 1 and 2), resulting in the promotion of a warm night (~18-20°C) instead of a cold night (10-15°), for a total of 7 days, affected the initiation of the second temperature-dependent delay term of the model (see Chapter 3). However, when the relevant days for South Africa were amended to mimic cold nights, the same as the minimum temperatures recorded at the field site, instead of a warm night, as originally indicated by the meteorological station data, model predictions improved. Mortality was predicted to take 53 days (a 1 day difference when compared with mortality estimates in Chapter 3, Table 4), which resulted in a 6 day error instead of 30. Although, differences in minimum temperatures were also high in Australia they resulted in the expression of a cold night to one that was colder (i.e. Ta = 16°C to Ta=8°C), hence, in this case the second delay term would have already been invoked and further night-time cooling would make no additional difference. Minimum temperatures have also been shown to be crucial in the accuracy of other climate based phenology model predictions (Jarvis & Stuart, 2001c; Jarvis & Collier, 2002).

Recalibrated body temperature models were most accurate for *L. pardalina, D. maroccanus* and *C. terminifera*. For *O. senegalensis* maximum body temperatures achieved throughout daylight hours tended to be underestimated resulting in differences in model and field mortality estimates in 1995 and 1996. There are a

number of potential sources of error for this species. The number of body temperatures recorded for *O. senegalensis* is fewer than that for the other three species above (see Chapter 2). They were also recorded over a much shorter period of time (4 days as opposed to a minimum of 10 days) over a smaller range of ambient temperatures (Blanford *et al.,* 1998). The higher T_{infl} for *O. senegalensis* indicates that maximal body temperatures and the initial delay term in the performance model (the second delay term is never invoked for *O. senegalensis* because of the warm nights), will not occur until relatively high ambient temperatures. This is likely to result in the variation in model output to field recorded mortality (Table 4 and 5).

Although, the availability of reliable data in some regions is a limitation, it should not discourage the use of this model to identify potential areas where this biopesticide can be used. There is a sufficient body of evidence whereby GIS has and is currently being used to identify "hotspots" critically in need of aid using climate data that are at the same resolution and/or at a coarser temporal and spatial scale. For example, targeting critical malaria areas most in need of bed nets (see Craig *et al.,* 1999; Martin *et al.,* 2002); predicting potential geographical distribution of non-indigenous pests (see Baker *et al.,* 2000); vulnerability of human and animal health to parasites (Sutherst, 2001); and conservation of ecological niches (Peterson *et al.,*1999, 2002).

The spatial model presented here has several advantages over single point site-specific evaluations. It allows for multi-point analyses to be made simultaneously with mapped outputs illustrating the spatial variability in the virulence of *M. anisopliae* var. *acridum* in controlling locusts and grasshoppers. Thus, allowing for pathogen performance assessments to be made between discrete locust and grasshopper populations within the same region, as illustrated in Spain and South Africa. The models are linked to meteorological station data, thereby capturing thermal ecology of the host and, thus overcoming differences in temperatures recorded at meteorological stations from those occurring at the field site. Not only can these models be used to make accurate predictions [also illustrated in the work by Bryant *et al.,* 2002 on the distribution of butterflies] but they can be used to investigate pathogen performance against the same species in different geographic locations (e.g. *N. septemfasciata* in Zambia and Mozambique) and against new and existing pest species, that are known active behavioural thermoregulators with similar

preferred body temperatures to *L. pardalina* or *C. terminifera* or *D. maroccanus*, such as *S. gregaria* in Mauritania.

The models can be used to investigate the average performance of the pathogen within a region based on historical data. Mortality predictions can be used to investigate the potential use of this biopesticide in new regions, such as in Spain, where *Metarhizium* is currently being investigated, as an alternative to chemical pesticides against *D. maroccanus* (see Chapter 1 and Chapter 5). The *Metarhizium*–based biopesticide has not yet been extensively used in this region, so the model could be used to perform a prospective analysis to determine likely efficacy and identify management strategies that will allow for the successful uptake of this product.

Tables and Figures

Table 1: Summary of overall accuracy between observed and estimated hourly temperatures derived using daily minimum and maximum temperatures collected at the field site for four locations: Niger, Zambia, South Africa, Spain and Australia. The intercept (a) and the slope (b) of the regression line, coefficient of determination (R^2), absolute mean error (AME) and root mean square error (RMS).

Country	***Field Temperature***				
	a	***b***	***R^2***	***AME*±(SE) *(°C)***	***RMS (°C)***
Niger	-0.641	1.035	0.98	0.816 (0.281)	1.096
Zambia	-0.410	1.057	0.84	1.251 (0.279)	1.963
South Africa	1.394	0.958	0.96	1.317 (0.320)	1.759
Spain	1.285	0.975	0.95	1.661 (0.391)	2.291
Australia	0.756	0.971	0.97	1.147 (0.089)	1.578

Table 2: Body temperature model parameter estimates for the sigmoid method (and asymptotic standard errors) for *Locustana pardalina*, *Dociostaurus maroccanus, Oedaleus senegalensis, Nomadacris septemfasciata, Chortoicetes terminifera* and *Model A.* Parameter estimates are based on simulated meteorological ambient temperature.

Species	***Habitat***	***Daily diurnal temperature range***	***Station Name (No.) Country***	***Model parameters***			
				Tmax (±SE)	***T_infl (±SE)***	***s (±SE)***	***R^2***
L. pardalina	Short-grass, exposed soil surface	16-32°C	Marydale (685270) South Africa	40.662 (0.348)	22.778 (0.216)	-6.964 (0.481)	**0.60**
D. maroccanus	Short-grass, exposed soil surface	16-32°C	Badajoz (83300) Spain	40.179 (0.234)	19.934 (0.152)	-5.97 (0.238)	**0.87**
O. senegalensis	Short-grass, exposed soil surfaces	24-34°C	Maine-Saroa (610960) Niger	41.975 (0.773)	29.634 (0.533)	-8.456 (1.174)	**0.56**
N. septemfasciata	Humid areas, long-grass wetlands	20-28°C	Lusaka (676650) Zambia	37.355 (0.449)	26.604 (0.798)	-3.952 (0.510)	**0.63**
C. terminifera	Short-grass, exposed soil surface	11-31°C	Hay (946980) Australia	41.179 (0.456)	19.416 (0.162)	-7.542 (0.559)	**0.73**
Model A	Short-grass, exposed soil surface	11-32°C	As above for *L. pardalina, D. maroccanus, C. terminifera*	39.194 (0.175)	21.330 (0.106)	-7.994 (0.341)	**0.64**

Table 3: Summary of overall accuracy of species-specific body temperatures between estimated hourly body temperatures derived using temperatures collected at the field site and simulated hourly temperatures from daily minimum and maximum meteorological temperatures (parameters obtained from Table 2) for five species: *O. senegalensis* (Niger), *N. septemfasciata* (Zambia), *L. pardalina* (South Africa), *D. maroccanus* (Spain), *C. terminifera* (Australia) and the generalised Model A. The intercept (a) and the slope (b) of the regression line, coefficient of determination (R^2), absolute mean error (AME) and root mean square error (RMS) are reported.

Species Country	***Field Temperature***				
	a	***b***	***R^2***	***AME*±(SE) (°C)**	***RMS (°C)***
O. senegalensis *Niger*	-0.226	0.947	0.90	2.168 (0.083)	2.783
N. septemfasciata *Zambia*	0.932	0.925	0.70	2.320 (0.181)	2.859
L. pardalina *South Africa*	4.244	0.859	0.88	2.022 (0.122)	2.960
D. maroccanus *Spain*	0.260	1.003	0.90	1.853 (0.101)	2.894
C. terminifera *Australia*	1.345	0.888	0.92	2.272 (0.129)	3.152
Model A	2.424	0.902	0.88	2.150 (0.052)	3.016

Table 4: Comparison of *Metarhizium anisopliae* var. *acridum* predictions made using meteorological station data in a GIS and mortality recorded in the field for locations where site-specific field temperature data were collected. The species include: *Oedaleus senegalensis* (1996, 1997), *Locustana pardalina* (1998), *Dociostaurus maroccanus* (2000), *Nomadacris septemfasciata* (2001) and *Chortoicetes terminifera* (2000).

Species	***90% Mortality (Days)***			***Source***
	Observed Field ST_{90}	***GIS ST_{90}***	***Residual (Observed – GIS)***	
O. senegalensis				
1996	21	16	-5	Langewald *et al.,* 1999
1997	15	15	0	Langewald *et al.,* 1999
L. pardalina				
1998	59	30	-29	Arthurs & Thomas, 2000
D. maroccanus				
2000	41	43	2	Based on model predictions using field data - see Chapter 3
N. septemfasciata				
2001	10	10	0	Pers comm. Elliot, S.L, Imperial College (see Chapter 3)
C. terminifera				
2000	19	18	-1	Pers. Comm. David Hunter, Australian Plague Locust Commission. Agriculture, Fisheries and Forestry – Australia

Note: Residuals that are positive suggest that the model predicts a slower speed of kill and negative suggests that the model under predicts a faster speed of kill.

Table 5: Comparison of *Metarhizium anisopliae* var. *acridum* predictions made using meteorological station data in a GIS and mortality recorded in the field for *Oedaleus senegalensis* during 1995, *Locustana pardalina* during 1995, *Schistocerca gregaria* during 1995 and *Nomadacris septemfasciata* during 1997.

Species	***90% Mortality (Days)***			***Source***
	Observed Field ST_{90}	***GIS ST_{90}***	***Residual (Observed – GIS)***	
O. senegalensis				
Niger, 1995	21(80%)	16	-5	Kooyman *et al.,* 1997
L. pardalina				
South Africa, 1995	20	25	5	Price *et al.,* 1997
S. gregaria				
Mauritania, 1995	15	17	2	Langewald *et al.,*1997
N. septemfasciata				
Mozambique, 1997	9	9.5	0.5	Price *et al.,* 1999

Note: Residuals that are positive suggest that the model predicts a slower speed of kill and negative suggests that the model under predicts a faster speed of kill.

Figure 1: Change in ambient temperature over height in comparison to temperatures recorded at the closest meteorological station. Ambient temperature at the soil surface (——), mean ambient temperature (——), ambient temperature at 30cm above the soil surface (-----), and simulated hourly temperature (—▲—▲—) using the Parton & Logan (1981) model with parameters representative of ambient temperature at 1.5m above the soil surface (a = 1.8, b=2.2, c=0.88 (Reicosky *et al.*, 1989)).

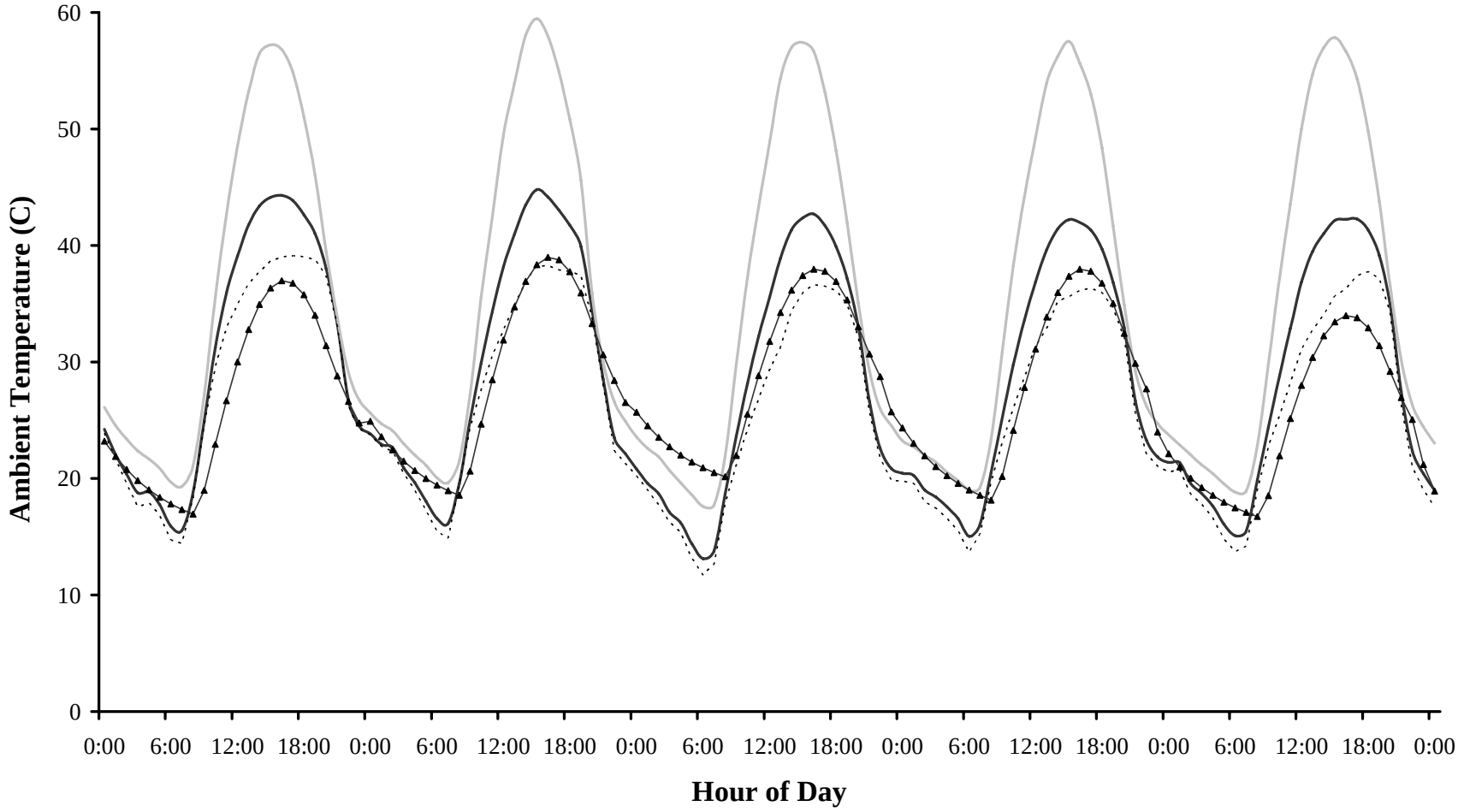

Figure 2: Simulated daily temperature (minimum temperature = 10°C; maximum temperature = 40°C) using two sine-curve parameters representative of two different environments. Temperatures in environment A (——) with day length of 12hrs are described using parameters (a=2.5, b=2.2, c=-0.1), while those in environment B (——), with a day length of 12hrs are described using parameters (a=1, b=5, c=-0.1). The potential error of temperature estimation between the two environments is illustrated (▨).

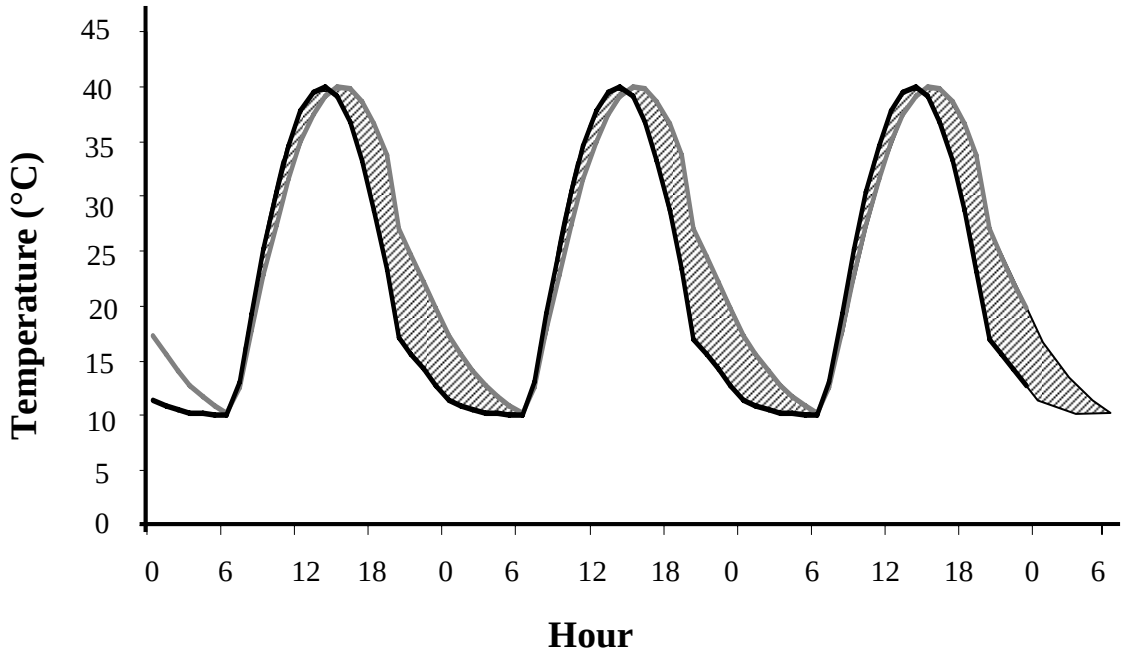

Figure 3: Maps illustrating the topography and distribution of meteorological stations, as a function of the total number of days missing temperature data for a single month, throughout the study regions; (a) West Africa (including Niger, Benin and Mauritania); (b) Southern Africa (including Zambia, Mozambique and South Africa); (c) Spain and (d) Australia.

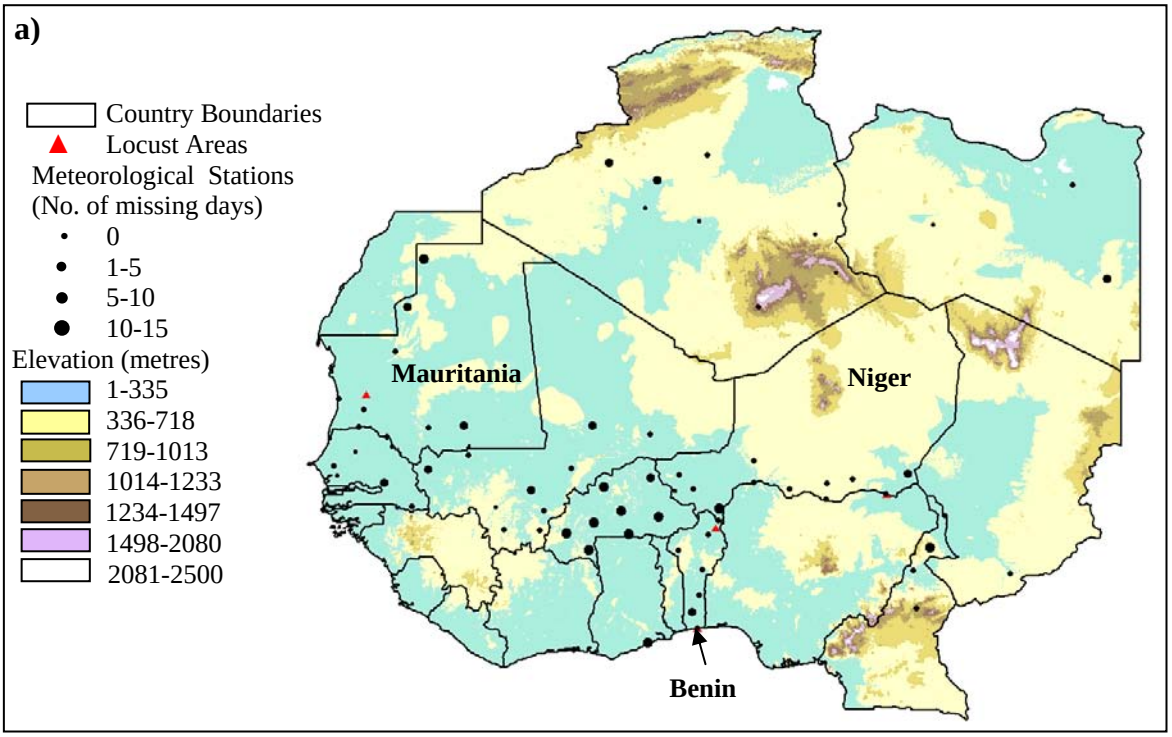

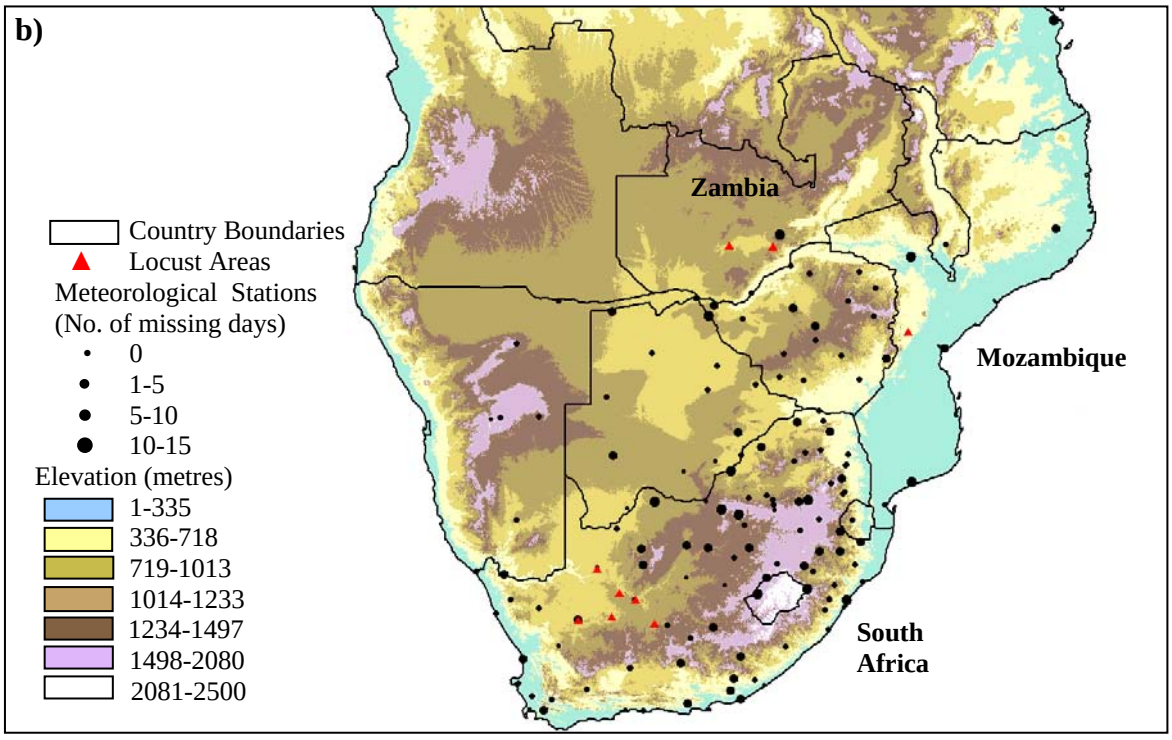

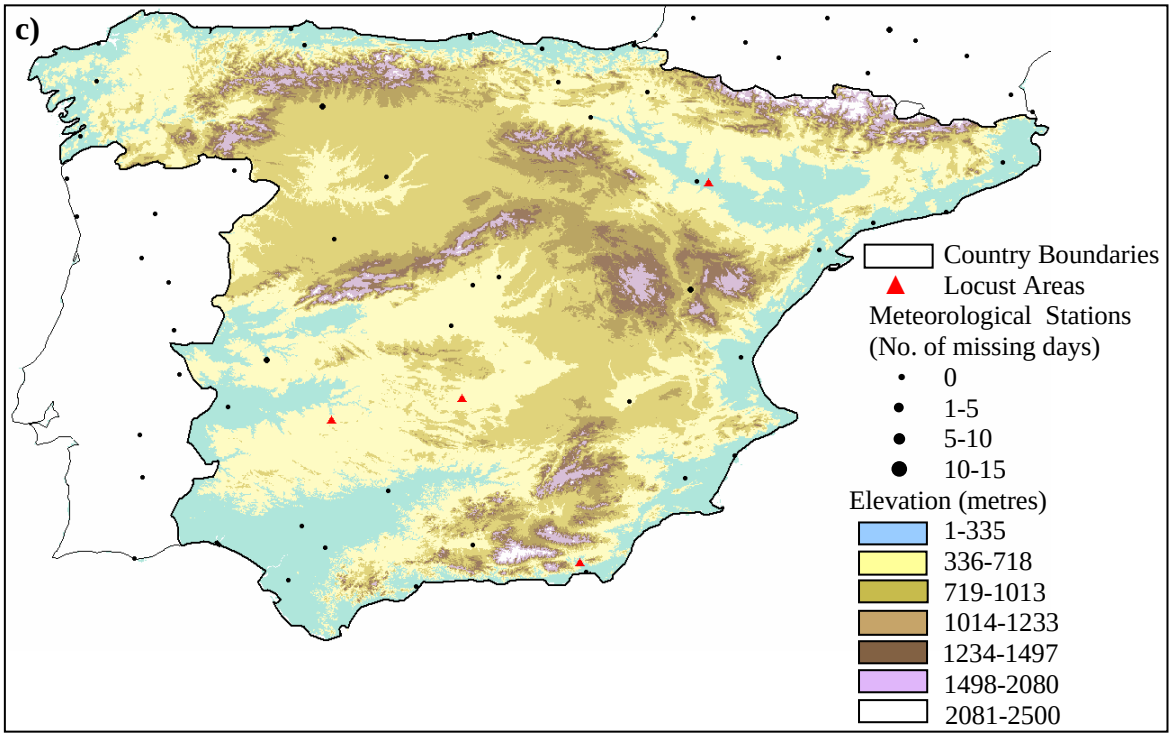
c)
Country Boundaries
Locust Areas
Meteorological Stations
(No. of missing days)
0
1-5
5-10
10-15
Elevation (metres)
1-335
336-718
719-1013
1014-1233
1234-1497
1498-2080
2081-2500

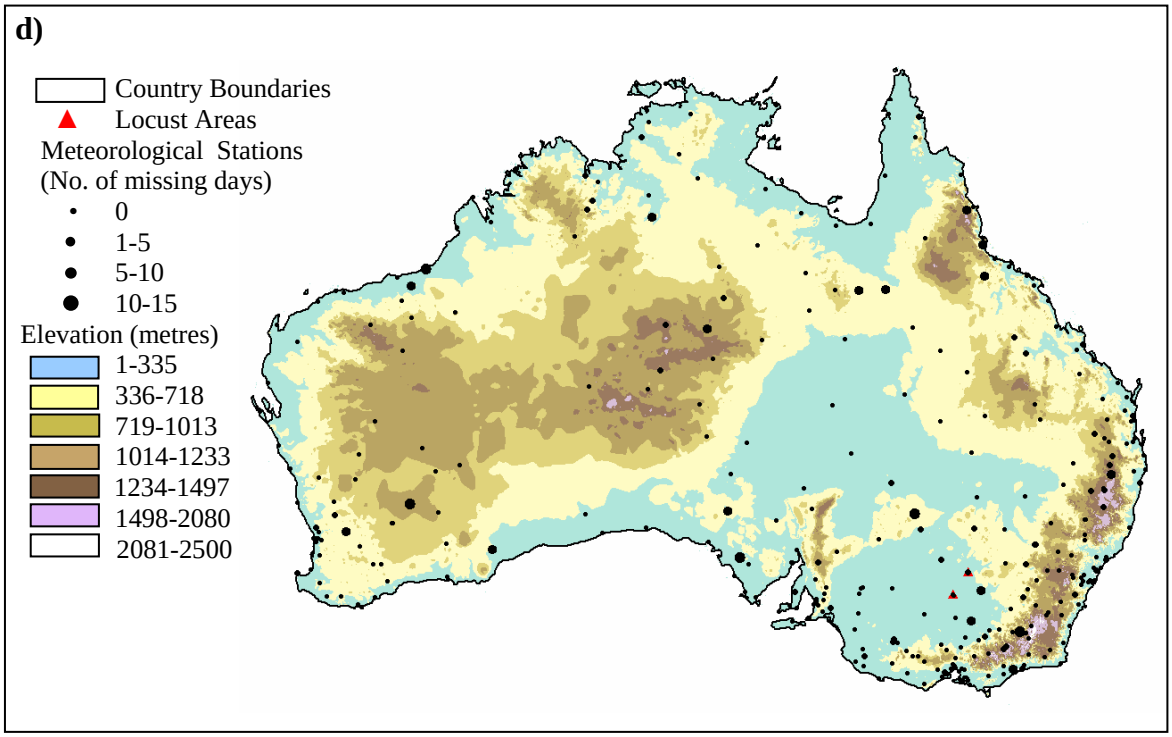
d)
Country Boundaries
Locust Areas
Meteorological Stations
(No. of missing days)
0
1-5
5-10
10-15
Elevation (metres)
1-335
336-718
719-1013
1014-1233
1234-1497
1498-2080
2081-2500

Figure 4: Difference in daily minimum (x-axis) and maximum temperature (y-axis) between the field site and the nearest meteorological station. Points represent differences in temperatures recorded in Niger, South Africa, Zambia, Spain and Australia. Positive values indicate that the temperatures recorded at the field site were greater than those at the meteorological station. Negative values indicate that temperatures recorded at the meteorological station were greater than those at the field site.

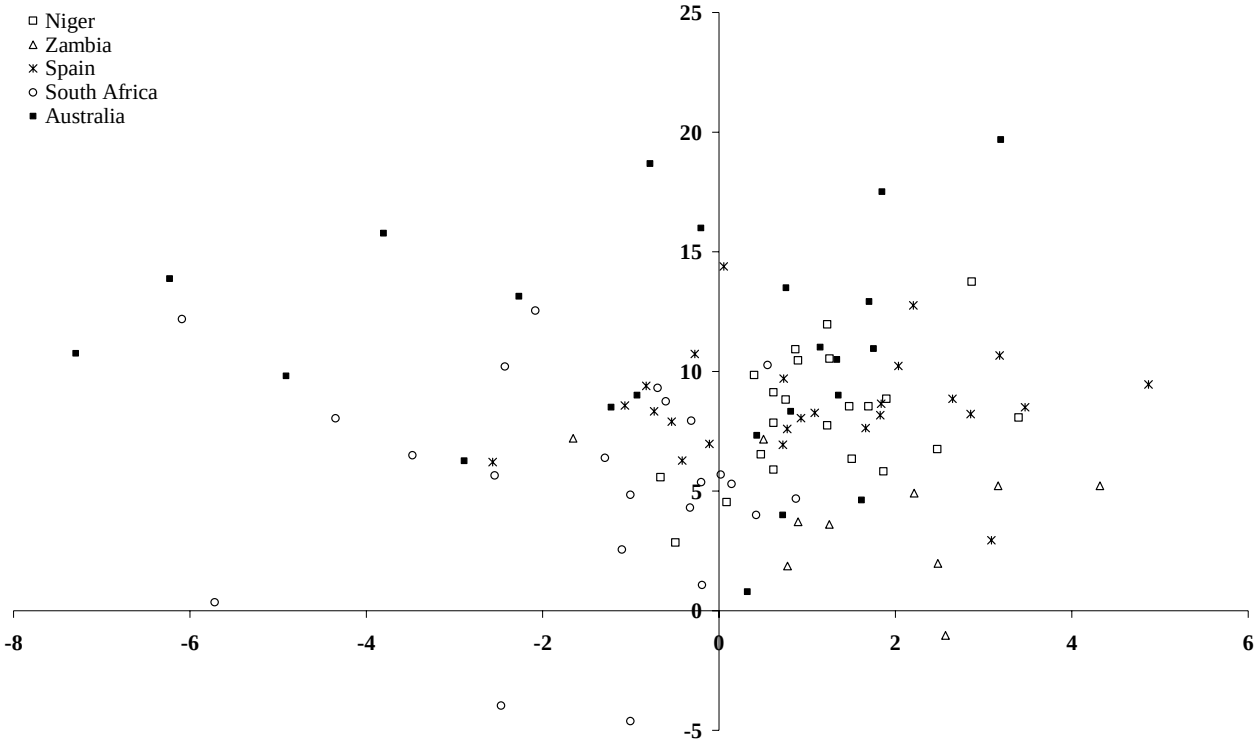

Figure 5: Mean hourly ambient temperature collected over four days at the field site (____) are plotted against simulated hourly ambient temperatures derived using daily minimum and maximum ambient temperatures collected at the field site (————) and simulated hourly temperatures derived using minimum and maximum temperature collected at a meteorological station (-----). Simulated temperatures were derived using sine-curve parameters: (a) Niger (a=1, b=5, c=-0.1), (b) Zambia (a=1, b=5, c=-0.1), (c) South Africa (a=1, b=1, c=-0.1), (d) Spain (a=2.5, b=2.2, c=-0.1), (e) Australia (same as South Africa).

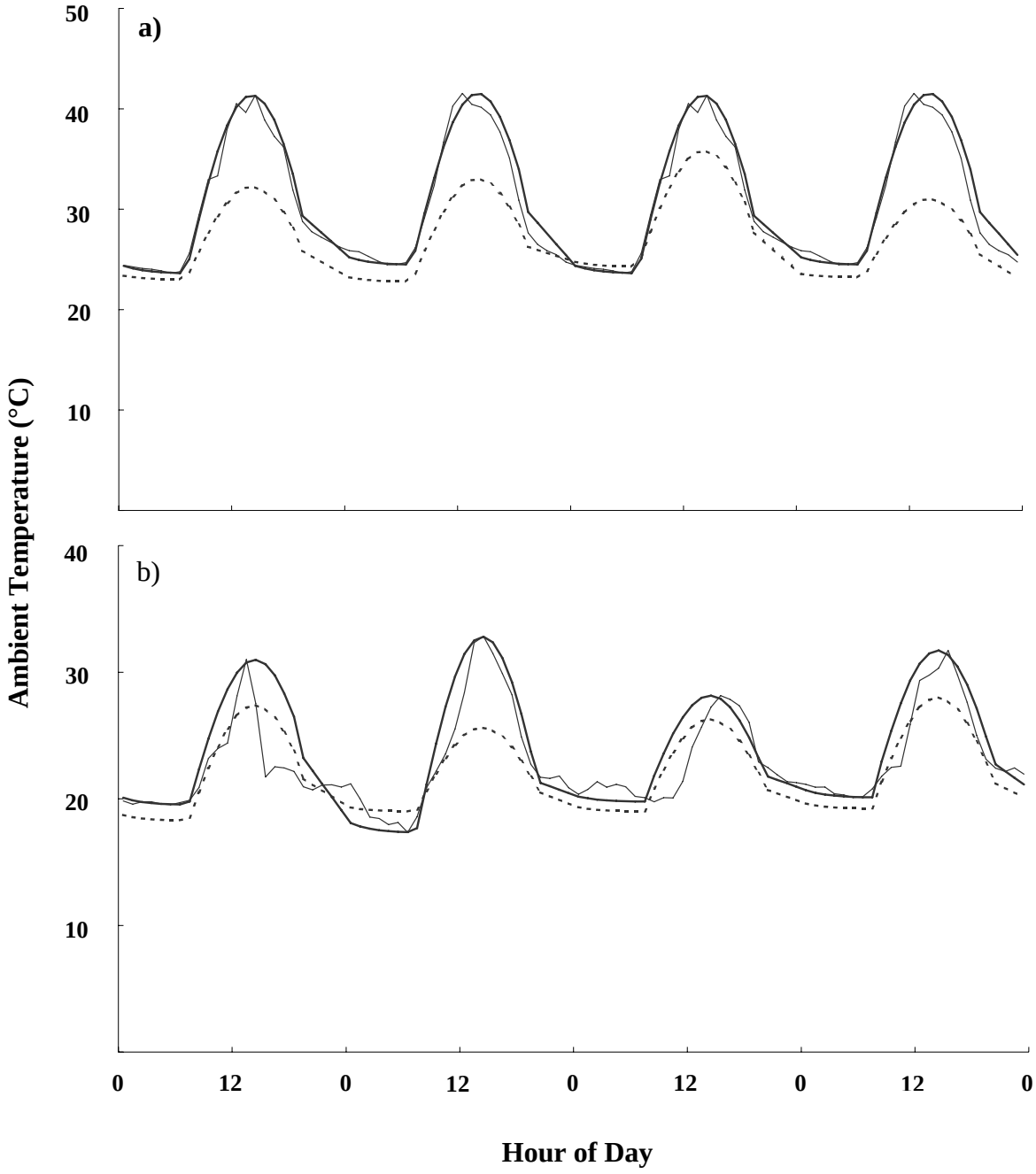

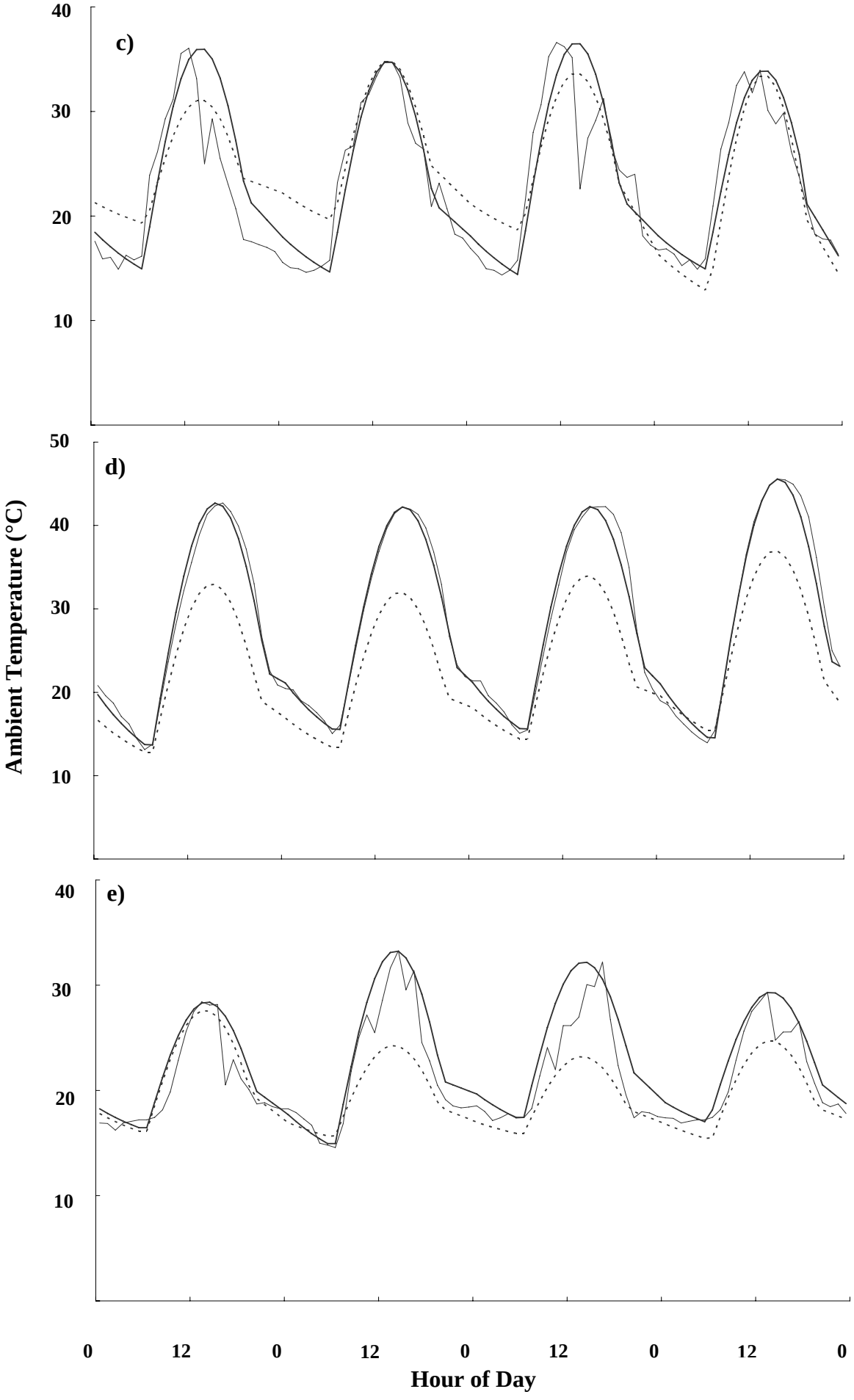
c)
d)
e)
40
30
20
10
50
40
30
20
10
40
30
20
10
Ambient Temperature (°C)
0
12
0
12
0
12
0
12
0
Hour of Day

Figure 6: Distribution of body temperatures (*Tb*) against ambient temperatures (*Ta*) for (a) *Oedaleus senegalensis*, (b) *Nomadacris septemfasciata*, (c) *Locustana pardalina*, (d) *Dociostaurus maroccanus* and (e) *Chortoicetes terminifera*. The straight line (———) shows a null model for no active thermoregulation whereby *Tb* = *Ta*. Best-fit body temperature regression curves (———) for individual species were derived using the parameters in Table 2.

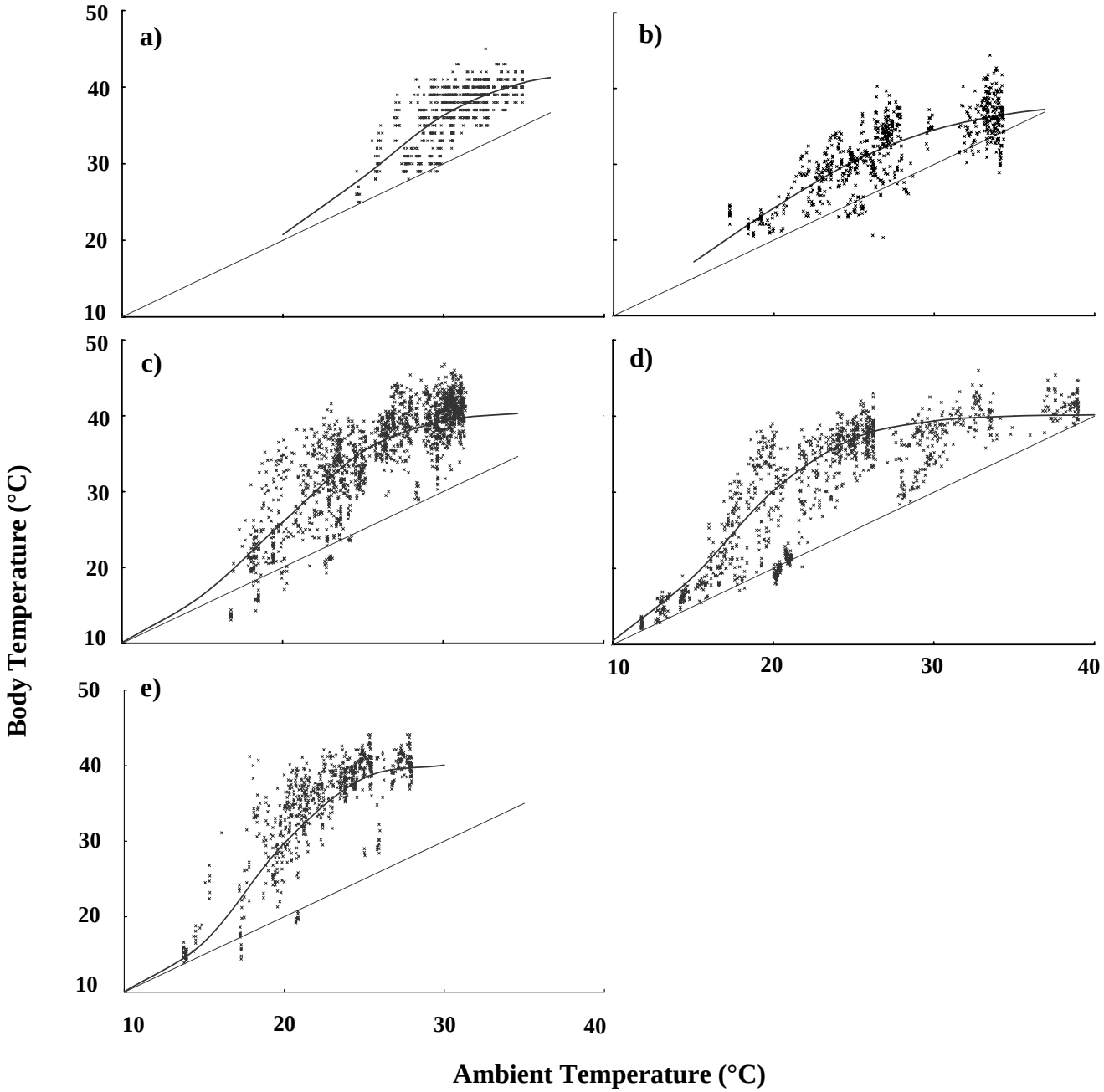

Figure 7: Mean hourly ambient temperature collected over four days at the field site (**- - - -**) is plotted with the predicted hourly body temperatures (————) using parameters from Chapter 2. For comparison, simulated hourly ambient temperatures derived using daily minimum and maximum ambient temperatures collected at meteorological stations (**—□—□—**) and recalibrated hourly body temperature predictions (—▲—▲—) from Table 2 for (a) *Oedaleus senegalensis,* (b) *Nomadacris septemfasciata* (c) *Locustana pardalina,* (d) *Dociostaurus maroccanus,* and (e) *Chortoicetes terminifera.*

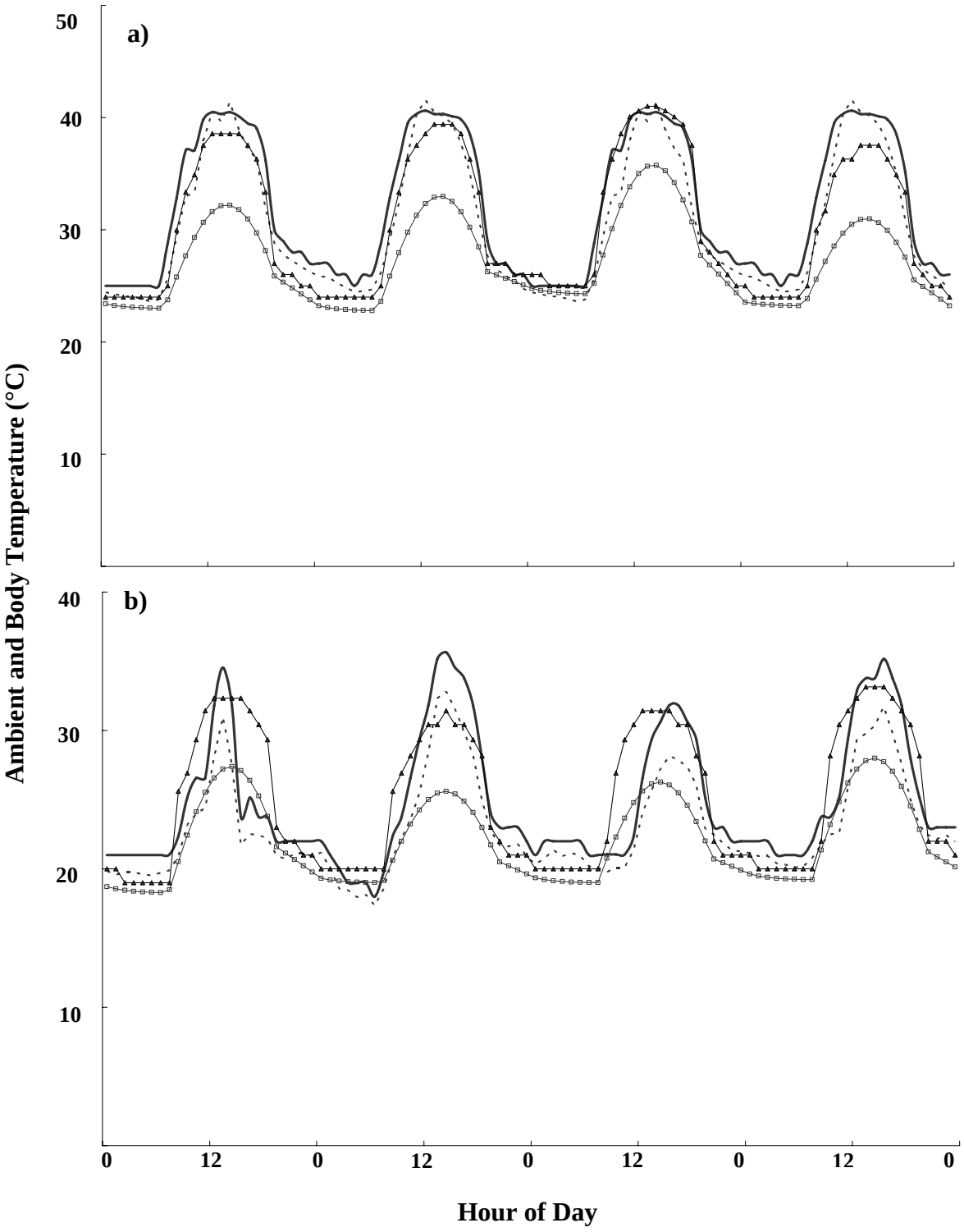

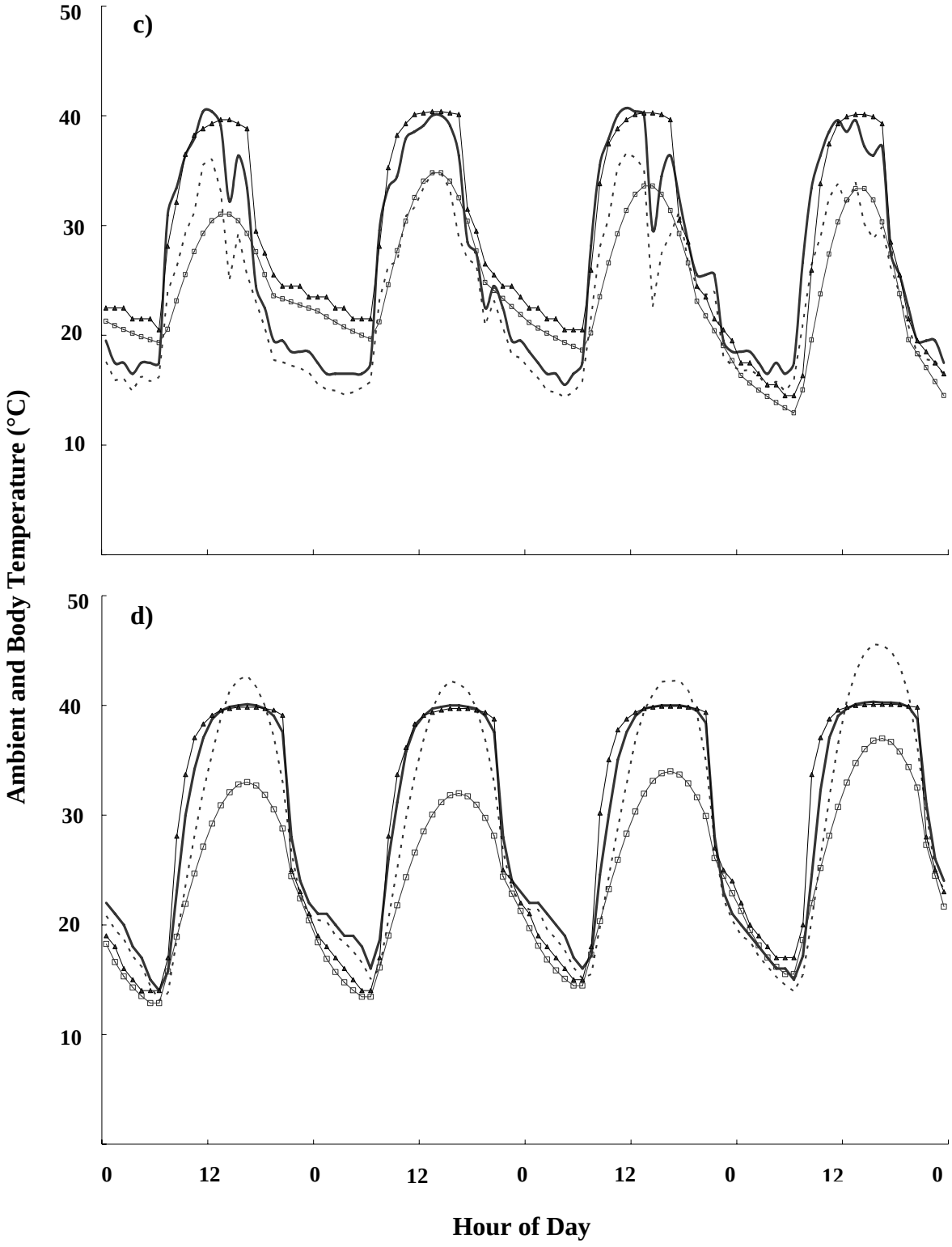
c)
d)
50
40
30
20
10
0
12
Ambient and Body Temperature (°C)
Hour of Day

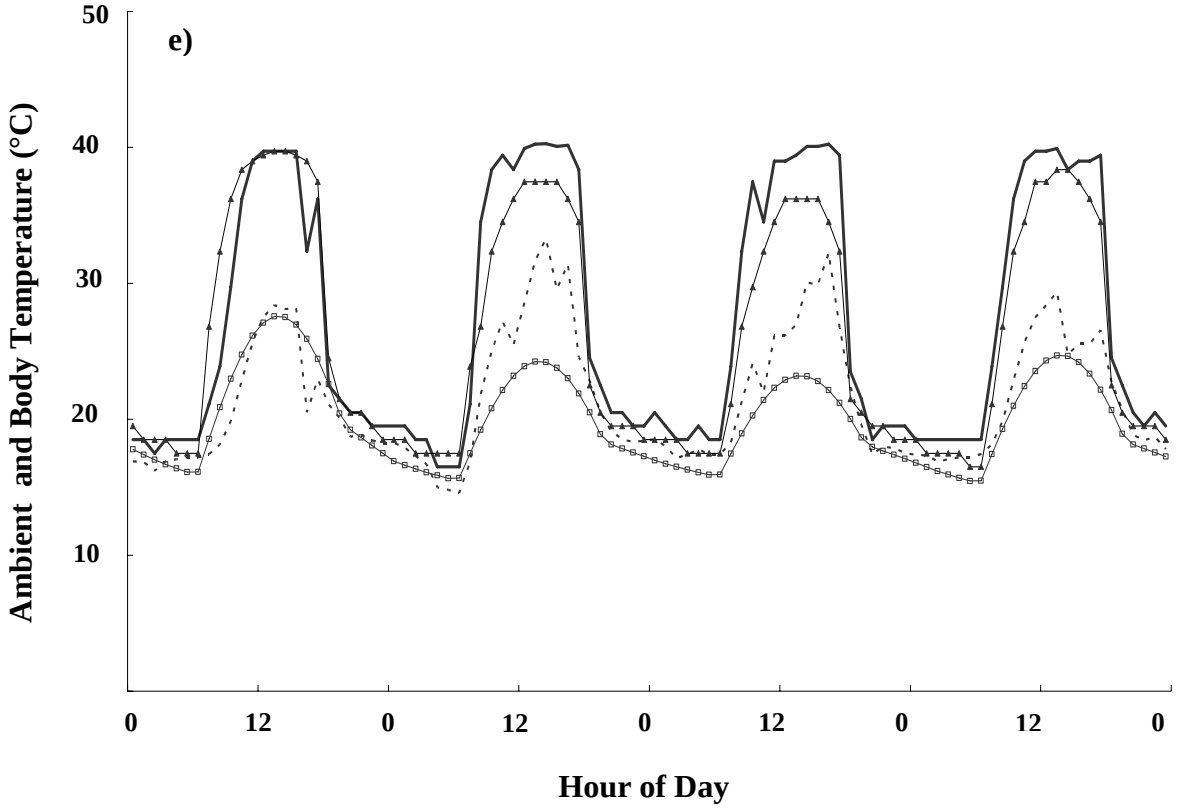
e)
50
40
30
20
10
Ambient and Body Temperature (°C)
0
12
0
12
0
12
0
12
0
Hour of Day

Figure 8: Mapped outputs illustrating the time taken to achieve 90% mortality by *Metarhizium anisopliae* var. *acridum* against (a) *Oedaleus senegalensis* in Niger. Simulations were run for 30 days starting on 17th August 1996; (b) *Nomadacris septemfasciata* in Zambia. Simulations were run for 20 days starting on 10th February, 2001; (c) *Locustana pardalina* in South Africa. Simulation was started on 25th February 1998 and run for 60 days; (d) *Dociostaurus maroccanus* in Spain. Simulations were run for 30 days starting on 25th May, 2000 and (e) *Chortoicetes terminifera* in Australia. Simulation was run for days starting on 7th November, 2000.

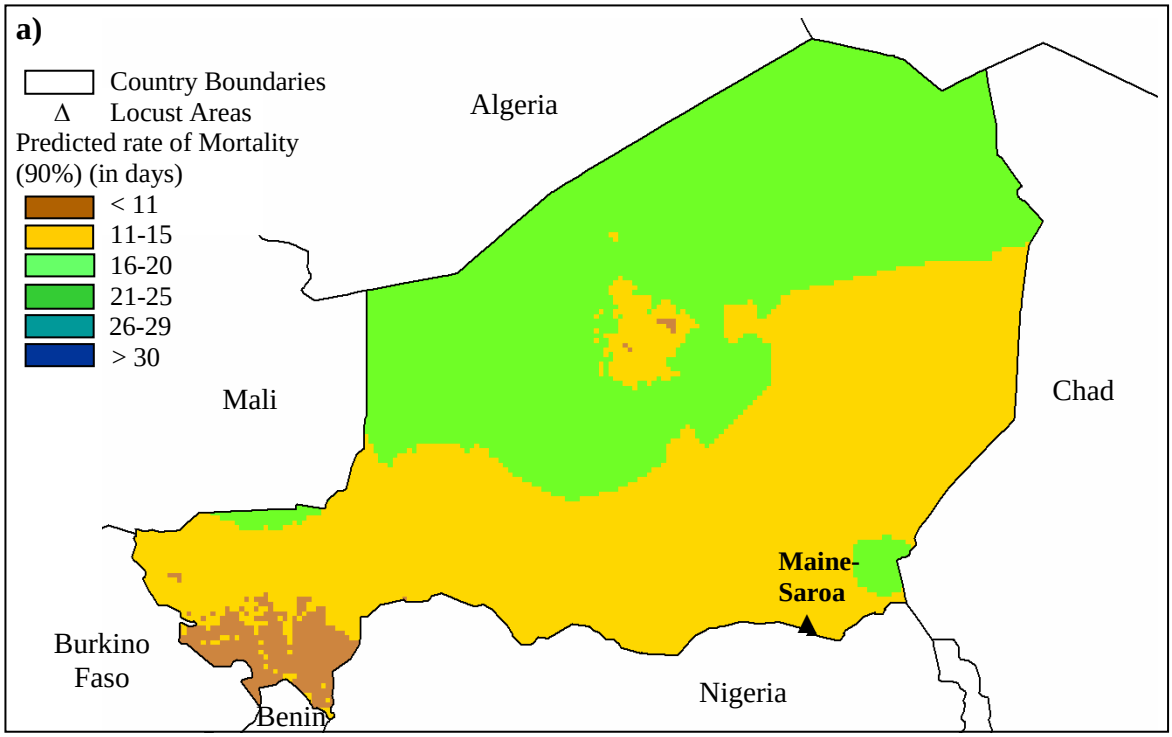

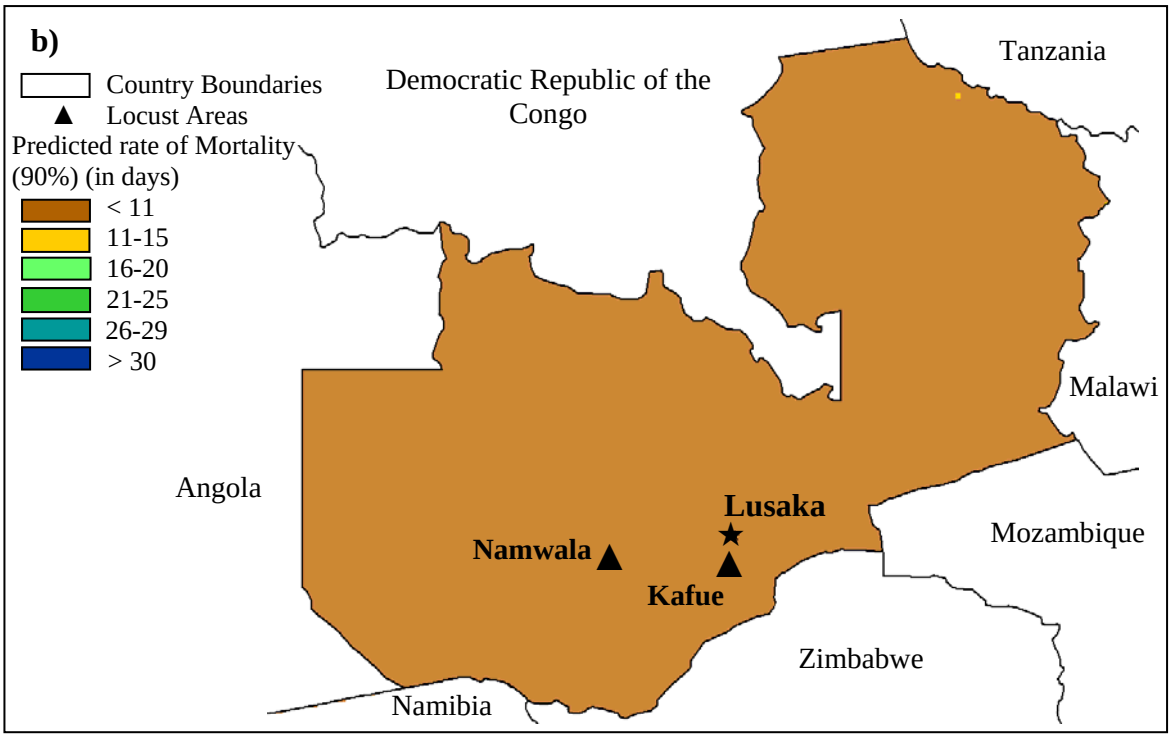
b)
Country Boundaries
Locust Areas
Predicted rate of Mortality (90%) (in days)
< 11
11-15
16-20
21-25
26-29
> 30
Democratic Republic of the Congo
Tanzania
Malawi
Angola
Lusaka
Namwala
Kafue
Mozambique
Zimbabwe
Namibia

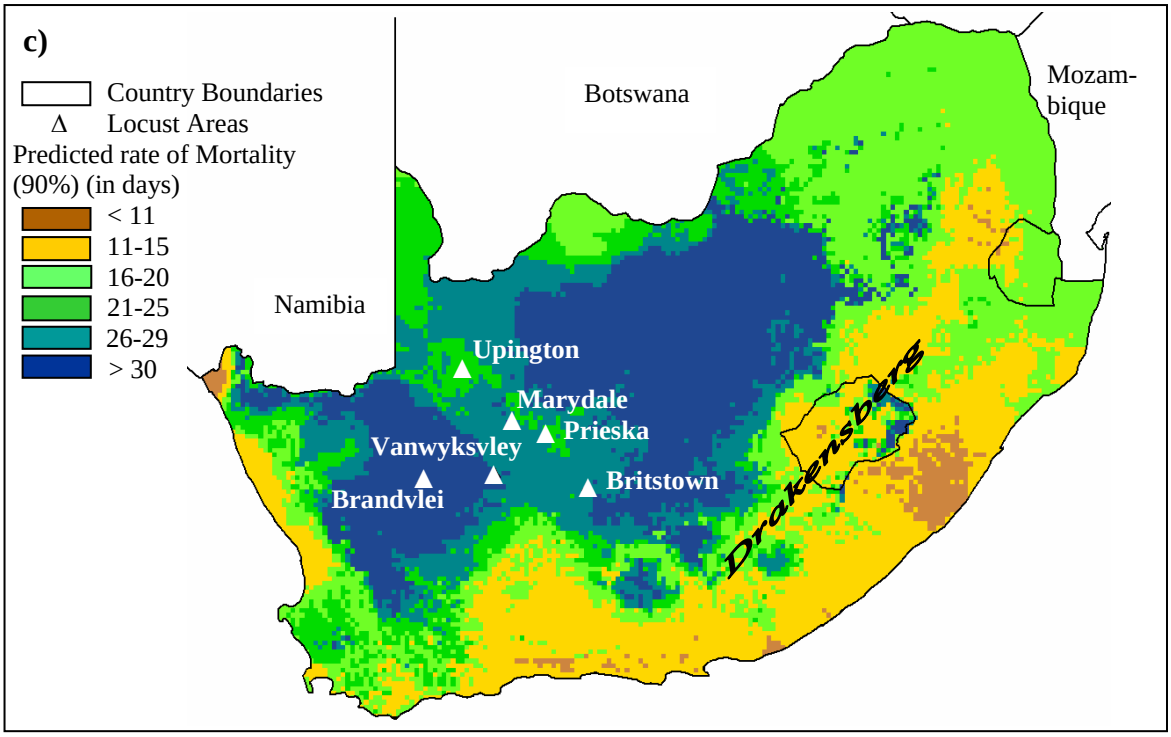
c)
Country Boundaries
Locust Areas
Predicted rate of Mortality (90%) (in days)
< 11
11-15
16-20
21-25
26-29
> 30
Botswana
Mozam-bique
Namibia
Upington
Marydale
Prieska
Vanwyksvley
Britstown
Brandvlei
Drakensberg

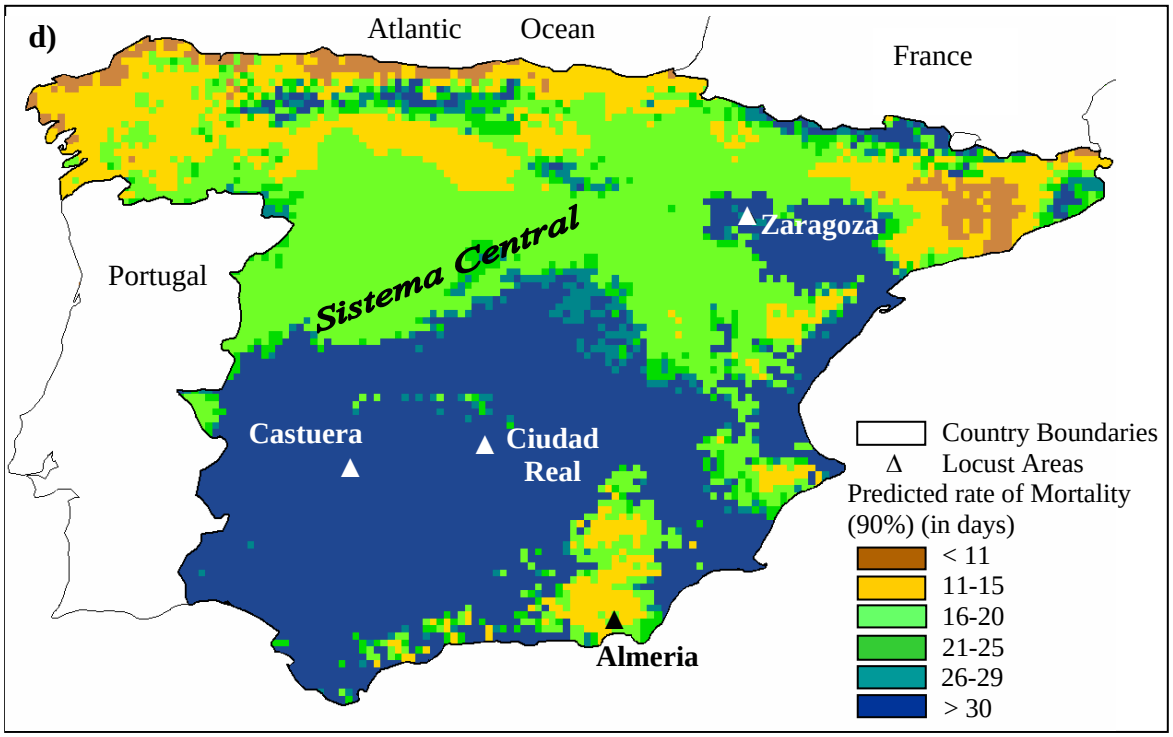
d)
Atlantic Ocean
France
Portugal
Sistema Central
Zaragoza
Castuera
Ciudad Real
Almeria
Country Boundaries
Locust Areas
Predicted rate of Mortality (90%) (in days)
< 11
11-15
16-20
21-25
26-29
> 30

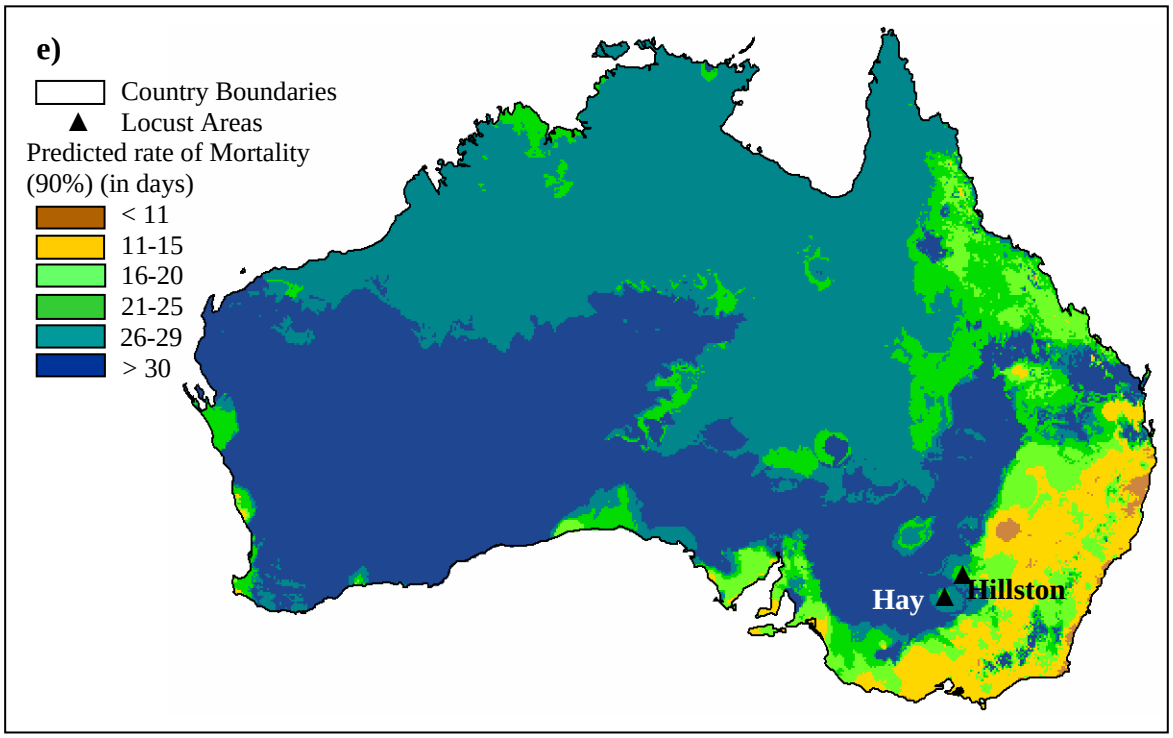
e)
Country Boundaries
Locust Areas
Predicted rate of Mortality (90%) (in days)
< 11
11-15
16-20
21-25
26-29
> 30
Hay
Hillston